Integrative Biology

Accepted Manuscript

ROYAL SOCIETY OF CHEMISTRY

www.rsc.org/ibiology

Insight, innovation and integration

A large body of evidence indicates a link between cellular mechanical features, neoplastic transformation and metastatic properties. Here we present a new optofluidic device able to analyze cellular deformability on the basis of the pressure needed to push a cell through a narrow constriction. This chip was capable to distinguish between cells with different metastatic potential and to highlight cell-response to drug treatments, using a small number of cells and in a short time. We expect that this device will enable a fast and highly efficient analysis of cancer cells, providing insights into the *status* of cell specimens in relationship to the transformation process and drug response.

Graphical and textual abstract

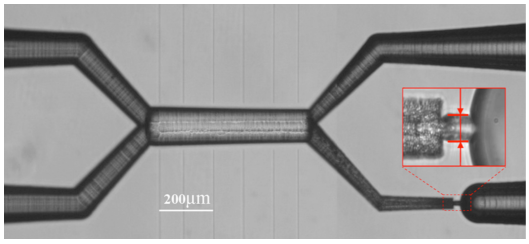

We present a new optofluidic device with a calibrated microconstriction for the analysis of cellular deformability.

Integrative Biology

RSCPublishing

ARTICLE

Optofluidic constriction chip for monitoring metastatic potential and drug response of cancer cells

Cite this: DOI: 10.1039/x0xx00000x

R. Martinez Vazquez[a†], G. Nava[b†], M. Veglione[c†], T. Yang[b], F. Bragheri[a], P. Minzioni[b], E. Bianchi[a], M. Di Tano[c], I. Chiodi[c], R. Osellame[a], C. Mondello[c*] and I. Cristiani[b]

Received 00th January 2012,
Accepted 00th January 2012

DOI: 10.1039/x0xx00000x

www.rsc.org/

Cellular mechanical properties constitute a good marker to characterize tumor cells, to study cell population heterogeneity and to highlight the effect of drug treatments. In this work, we describe the fabrication and validation of an integrated optofluidic chip capable of analyzing cellular deformability on the basis of the pressure gradient needed to push a cell through a narrow constriction. We demonstrate the ability of the chip to discriminate between tumorigenic and metastatic breast cancer cells (MCF7 and MDA-MB231) and between human melanoma cells with different metastatic potential (A375P and A375MC2). Moreover, we show that this chip allows highlighting the effect on cancer cells of drugs interfering with microtubule organization (paclitaxel, combretastatin A-4 and nocodazole), which led to changes in the pressure-gradient required to push cells through the constriction. Our single-cell microfluidic device for mechanical evaluation is compact and easy to use, allowing for an extensive use in different laboratory environments.

Introduction

Cellular mechanical properties can be exploited as an inherent cell-marker for different pathologies and as a label-free criterion to define the health state of a cell. Indeed, several studies on cancer cells revealed a clear relationship between cellular transformation and mechanical properties, with an increase in cellular deformability from normal cells to tumorigenic and metastatic ones[1-4]. Cellular cytoskeleton, which consists in an intricate network of different protein filaments, namely actin filaments, intermediate filaments and microtubules[5], plays an important role in determining cellular mechanical properties. In fact, variations in cytoskeletal organization, either occurring spontaneously, as during malignant transformation, or induced by specific drugs, can be associated with changes in cellular physical properties[6-9].

Being cellular deformability a possible marker of cancer progression and drug response, the availability of devices able to investigate the mechanical behaviour of a cell population at the single cell level could give a valuable contribution to cancer diagnostics and cancer cell treatment. In this context, microfluidics has provided promising tools to manipulate and study mechanical properties of single cells, as it allows the integration, in a millimetre-scale device, of cells' selection and probing by different methods[10,11]. Many devices have been developed for studying viscoelastic properties of cells in microfluidic environments, among them the optical stretcher, which has the ability to deform cells without mechanical contact[12], and chips in which cells are pushed into narrow channels, which can well mimic cell *in vivo* behaviour[13,14]. In an optical stretcher the radiation impinging on the cell from two opposing sources (generally waveguides or fibers) produces a surface stress, yielding a cell deformation which can be controlled and measured by means of an optical microscope and a CCD camera[15]. This system allows, in principle, to evaluate different parameters of cell mechanical response to the applied stress, as both the static ("steady-state" deformation) and dynamic (deformation and recovery time-constants) parameters of cell mechanical response can be assessed.

On the other side, in microfluidic chips with calibrated micro-constrictions cells have to squeeze through the constriction, and this can happen either by leaving cells to migrate by themselves[16] or by applying an external pressure to force them to pass[17,18]. Commonly, the channel surfaces are pre-treated to avoid adhesion between cells and channel walls and the micro-constriction is long enough to allow the measurement of the time for entry and the cell migration speed as indexes of a cell's capacity to change its shape and migrate[19-21].

Here we propose a new approach in a constriction-based microfluidic chip consisting in the measurement of the

minimum pressure needed to make a cell pass through the constriction. The chip begins with an optical sorter, allowing the analysis of one cell at a time without the interference of the other cells in the sample; the sorter directs the cell under study from the continuous central flow to the constriction arm, avoiding clogging of the chip. When the cell reaches the constriction, the pressure applied at the chip input is increased linearly with time, while that at the output is not modified, until the cell passes through the constriction. Thanks to this approach a considerable reduction in measurement time is achieved, as now only few seconds for each cell are required instead of several minutes as in traditional microfluidic-constriction assays. Additionally, internal channel surfaces do not require any pre-treatment, thus simplifying chip usage and cleaning, and allowing for its reuse after each experiment.

In this paper, we demonstrate that this chip allows distinguishing different cancer cell lines depending on their metastatic potential. Moreover, by using drugs interfering with microtubule organization, we show that microtubules play an important role in controlling cell passage through the constriction and that the chip has a high capability to discriminate between treated and untreated cells. Our device is not designed to mimic *in vivo* behaviour of cancer cells but to give a reliable method to distinguish between cancer cells at different stages of tumor progression.

Methods and materials

Optical stretcher fabrication and measurements

Cell-stretching experiments were performed using a monolithic optical stretcher. This device was fabricated in a commercial microfluidic chip (Translume) by direct implementation of optical waveguides through femtosecond laser writing, as explained in detail elsewhere[22]. For stretching measurements, a cell suspension was injected into the optical stretcher chip and passed in a rectangular microchannel (100×250μm). A CW Yb-doped fiber laser (YLD-10, IPG Fibertech), with an emitting power up to 10 W at 1070 nm, was utilized as light source. Once a cell reached the region illuminated by the two counter-propagating beams (25 mW each), carried by the integrated optical waveguides, the cell was trapped at the channel center. The laser power was then increased to 1.2W per side for 5s, in order to stretch the cell, and the process was recorded by a CCD camera. By analysing the frames, it was possible to evaluate the deformation of each cell by measuring the variation of the ellipticity with laser power, according to the formula: deformation (%) = $100\times Corr\times(e_1-e_0)/e_0$, where e_1 is the ellipticity of a cell at the end of the stretching procedure and e_0 the same cell at the beginning of the measurement[7]; *Corr* is a correction term to compensate the different force distribution caused by different cell dimensions. Measurements were performed at room temperature and repeated at least twice on each cell line.

Constriction-chip design, fabrication and measurements

The schematic of the constriction chip is shown in Fig. 1a. The design is based on a double-Y-shaped channel: two input channels merge into a central section where cell sorting is performed by a light waveguide; the central section then separates into two output channels, one of which contains an elliptical 3D constriction for cell testing. As explained elsewhere[23], laminar flow is achieved in the central section and sorting is performed by optical forces that direct the cells into the desired output[24].

The optofluidic chip was entirely fabricated by femtosecond (fs) laser micromachining. In particular, the microfluidic network was created by fs laser irradiation followed by chemical etching (FLICE) and the waveguide just by fs laser irradiation, with parameters previously reported[25]. A detail of the irradiation for the fabrication of the constriction section is shown in Fig. 1b, an irradiated region is embedded between two non-irradiated ones that will afterwards constitute the constriction region. These non-irradiated regions slow down the etching process thus exposing the constriction region for a much shorter etching time. This results in a 3D elliptical section constriction with axial dimensions of 7 × 30 μm (y × z) and a length (x direction) of 15 μm (see Fig. 1c and 1d).

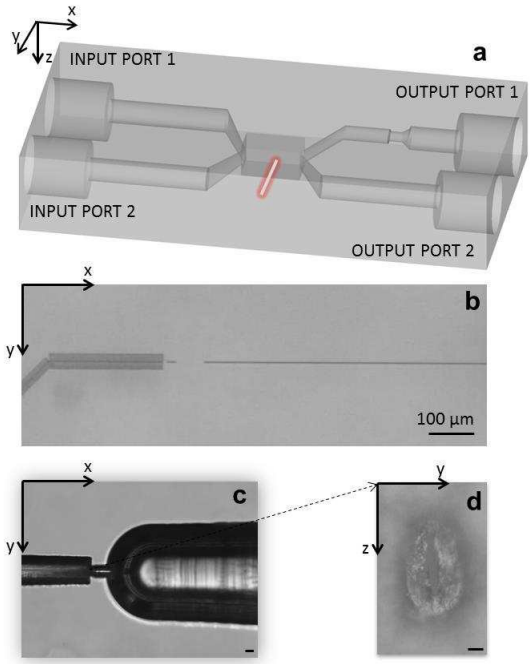

Fig.1 Constriction-chip characteristics. (a) 3D scheme of the constriction chip where the waveguide is highlighted in red; (b) microscopy image of the glass irradiation at the constriction region; (c) detail of the chip after etching in the x-y plane and (d) microscope image of the constriction (y-z plane). Scale bar dimension is 10 μm in both (c) and (d).

Thanks to the use of two computer-controlled micropumps, buffer solutions without and with cells (initial concentration 200 cell/μL) were injected at input ports 1 and 2 (pump pressure ≈ 10 mbar, flow-rate ≈ 150 nL/s), respectively and,

owing to laminar flow condition, two separate fluxes were obtained, even in the common central channel. Pressure levels were regulated so that, in steady conditions (≈ 1-2 mbar, flow-rate ≈ 15 nL/s), all cells remained in the original flux, passing through the constriction-less branch, and being delivered at output port 2. To direct a cell toward the constriction-branch, the laser emission in the central section, as indicated in Fig. 1a, was turned on (irradiating the cell with a laser power of 150 mW for a duration of 4 s) and the radiation pressure exerted on the selected cell moved it from the original flux to that made of pure-buffer fluid, thus passing through the constriction.

When the cell reached the constriction, and stopped at the constriction opening, a slow pressure-ramp (1 mbar/s) was applied to the input channels, thus increasing the force pushing the cell through the constriction. For each cell, the whole sequence was recorded at 15 frames per second by a CCD camera connected to the microscope, together with the pressure corresponding to each frame (see supplementary video) and the pressure increase required to push the cell through the constriction which has been defined as the cell specific "passing pressure" . With this chip, it is thus possible to send a single cell at the time to the constriction branch and to analyse the constriction-passing condition required by each specific cell. All the measurements were performed at room temperature (20±1ºC) and repeated at least twice for each cell line and for each treatment, analysing 50-70 cells/sample.

Cells lines, drug preparation and treatment

Two pairs of cancer cell lines characterized by different metastatic potential were used for the experiments: MCF7 and MDA-MB231 (non-metastatic and metastatic human breast carcinoma cells, respectively), and A375P and A375MC2 (metastatic and highly metastatic human melanoma cells, respectively) [26-28].

Cells were cultured in Petri dishes (Corning) and grown in Dulbecco's Modified Eagle's Medium (DMEM, Euroclone) supplemented with 10% Fetal Bovine Serum, penicillin (0.1 mg/ml, Euroclone) and streptomicin (100 U/ml, Euroclone), 0.2 mM glutamine and 1X non-essential aminoacid (Euroclone). Cells were maintained in an incubator at 37°C in a humidified atmosphere at 5% CO_2. For mechanical property analysis, 10^6 cells were plated in 10 cm Petri dishes, exposed to drugs when required, and detached by trypsinization about 24 hours after plating. Cells were then resuspended in culture medium without serum at a density of about 2×10^5 cells/ml, in order to ensure a regular presence of cells within the flow. On each cell sample prepared for mechanical property analysis, we determined the percentage of viable cells using the Trypan blue method. An aliquot of the cell sample was mixed in a 1:1 ratio with a 0.5% Trypan blue solution in PBS and cells were then counted using a burker chamber. Upon staining, dead cells appear blue, because their membrane became permeable to the dye; in contrast viable cells exclude the dye and appear white.

Paclitaxel (PTX), combretastatin A-4 (CA-4) and nocodazole were purchased by Sigma-Aldrich. Stock solutions (10 mM PTX, 20 mM CA-4, 33 mM Nocodazole) were prepared in DMSO, conserved at -20°C and diluted at the final concentration in complete medium for cell treatment. As cell size could interfere with the analysis of cellular mechanical properties, the cell size distribution of each population was determined by measuring the diameter of cells, either exposed or not exposed to drugs, inside the constriction chip. The average size was similar within each couple of cell lines and did not change significantly after drug treatment (Table S1). This allowed a direct comparison between the cell lines of each pair and between treated and untreated cells of the same cell line. Note that in all the lines, the cell diameter was high enough to completely clog the constriction in the y direction.

Wound healing and immunofluorescence experiments

For the wound healing assay, MCF7 and MDA-MB231 cells were plated in 3 cm Petri dishes at a concentration of 4.5×10^5 cells/dish. Cells were incubated for 24 hours at 37°C to reach confluence and, after removal of the medium, a wound was carefully made with a 1 ml micropipette tip on the cell monolayer. Images of three areas of each wound were acquired as a record of the initial wound size. Cells were then incubated at 37°C with or without the drug and images of the same wound's areas were taken to monitor cell movement. Images were acquired using an inverted optical microscope Olympus IX71, equipped with a 4X objective and a digital camera Cool SNAPS (Photometrics), driven by the "MetaMorph 7.7.5" software. The calculation of wound areas at time 0 and at the end of the incubation time was done on the digital images using "Adobe Photoshop CS5 Extended".

For immunofluorescence experiments, cells were seeded in 12 well plates (Corning) containing 18 mm diameter coverslips and incubated at 37°C for 24 hours. After drug treatment, cells were fixed with 100% pre-cooled methanol for 1 min, treated with 0.1% BSA in PBS for 30 min. and incubated with anti-α tubulin (clone DM1A, Sigma Aldrich) diluted 1:1000 in 0.1% BSA for 1 hour at room temperature. Cells were then incubated at room temperature with a TRITC conjugated anti-mouse secondary antibody (Jackson ImmunoResearch) diluted 1:100 in 0.1% BSA. Nuclei were counterstained with DAPI (4',6-diamidino-2-phenylindole). Slides were observed using an inverted Optical Microscope Olympus IX71, equipped with 60X objective and images were taken as described above.

Statistical tests

In order to evaluate the experimental data obtained on passing pressure, we performed a statistical analysis. We first applied a Kolmogorov–Smirnov test to evaluate if the experimental data could be considered as extracted by a normal distribution, and the results demonstrated that the distribution was not, generally, a normal one. This result pushed us to use a non-parametric test for the comparison of the data obtained by different

populations, and we thus decided to apply the Mann-Whitney U-test. Statistical analysis on the wound-healing assay was performed using the student's t-test.

Results and Discussion

Analysis of deformability and passage through the constriction of cell lines with different metastatic potential

As a preliminary experiment, by using the optical stretcher chip, we confirmed that cellular deformability increases with the increase of the metastatic potential. In fact, under the same operating conditions, metastatic MDA-MB231 cells were more deformable than not metastatic MCF7 cells (Fig. 2a), in agreement with the data of the literature[7], and A375MC2 were more deformable than the less metastatic A375P cells (Fig. 2b).

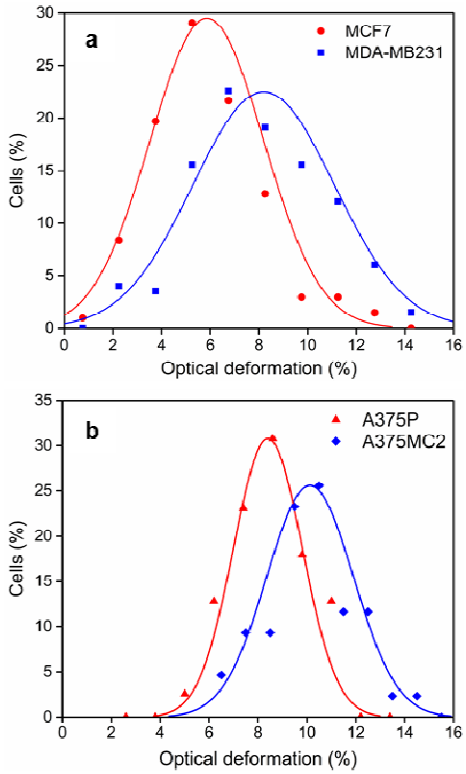

Fig.2 Optical deformation of (a) MCF7 and MDA-MB231 and (b) A375P and A375MC2 cells. Measurements were performed on about 200 cells of each cell line.

We then analysed the behaviour of the breast cancer cells with the constriction-chip. We found that passing pressures clearly separated the two cell populations as shown in Fig. 3a (detailed results on passing pressure values and statistical analysis results are reported in Table 1). Metastatic MDA-MB231 cells appeared more heterogeneous than MCF7, but most of the cells required higher pressures to pass through the constriction than MCF7 cells (Fig. 3a). In fact, the average passing pressure for MDA-MB231 was 13.0±6.7 mbar *vs.* 3.6±2.3 mbar for MCF7. Interestingly, the difference in the passing-pressure distributions is more evident than that observed between the two stretching-deformation distributions. The same type of result was obtained with melanoma cells (Fig. 3b). Again, the more metastatic cells (A375MC2) were more heterogeneous and required higher pressures than the less metastatic ones (A375P) to pass through the constriction (12.2±3.6 mbar *vs.* 8.3±2.1 mbar). Thus, the constriction-chip allows distinguishing cancer cells on the basis of their metastatic potential, which is positively related to the pressure required to pass through the constriction.

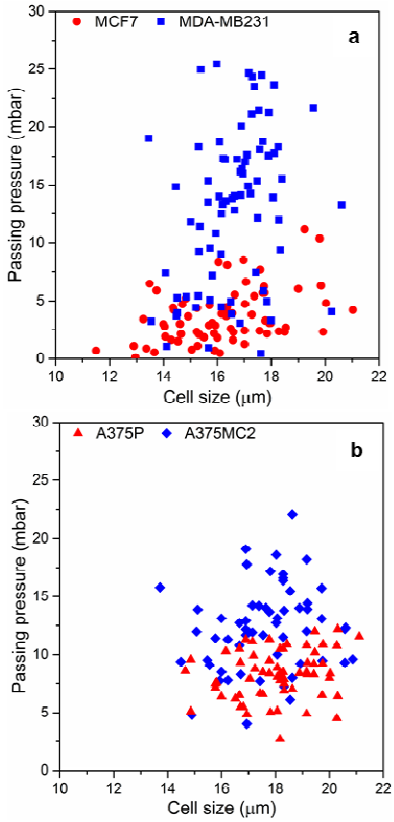

Fig.3 Analysis of MCF7 and MDA-MB231 (a) and A375P and A375MC2 cells (b) with the constriction chip. The cell size is plotted against pressure values required to push cells through the constriction.

Table 1. Experimental data for each plot reported in Fig. 3. The mean passing pressure with the standard deviation and the median passing pressure are reported for each cell line, together with p values of the statistical analysis (U-test).

Cell line	Passing pressure (mbar)		p value
	Mean ±SD	Median	
MCF7	3.6±2.3	3.1	<0.001
MDA-MB231	13.0±6.7	13.9	
A375P	8.3±2.1	8.4	<0.001
A375MC2	12.2±3.6	12.2	

In our device, the increased deformability of cancer cells with greater metastatic potential, demonstrated by the higher deformation obtained when cells are stretched with OS, is associated with the requirement of higher pressures to push

cells through the constriction. Although this behaviour seems counterintuitive, a qualitative explanation can be provided considering how cells pass through the constriction. When the cell under analysis arrives at the constriction, it is blocked at the entrance because of its size; subsequently, the cell deforms and squeezes into the constriction and then rapidly passes through it (see ESI video). The total force acting on the cell at the constriction results from the balance between pressure gradient and friction with the entrance walls (see Fig. 4). In a simplified model forces due to pressure gradient would push the cell through the constriction, but are contrasted by friction forces. As schematically shown in Fig. 4, the deformability of the cell is expected to have a role in determining the friction forces. In fact, more deformable cells tend to adhere on a larger glass surface surrounding the constriction entrance, thus opposing a greater resistance to sliding into the constriction. Moreover, it is worth noticing that the device is fabricated on a glass substrate and the channels walls are not treated, thus probably favouring cell adhesion to the constriction walls, with respect to polymer-based microfluidic circuits. In all cases, at a certain value, the pressure gradient is high enough to prevail and push the cell inside the constriction, but the required pressure will be higher for the more deformable, softer, cells.

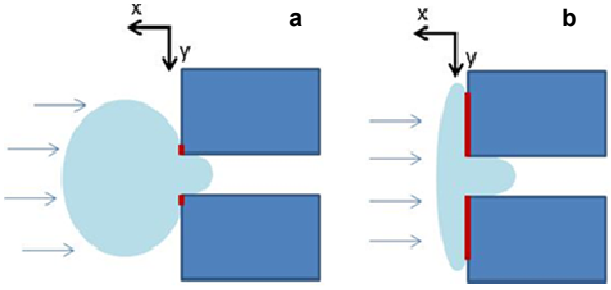

Fig.4 Schematic of the cell at the constriction entrance. (a) Less deformable and (b) more deformable cells, which adhere to the constriction entrance walls. The contact surface between the cell and the glass walls is highlighted in red.

Monitoring cancer cell response to drugs interfering with microtubule organization with the constriction chip

Microtubules are rigid cytoskeletal structures[29] involved in cellular motility and shape determination. Microtubule stabilizing or depolymerizing agents, altering microtubule subtly tuned organization, can impair cellular migration and have thus been proposed as possibly anti-angiogenic, anti-metastatic drugs[30]. Because these agents can also be expected to have an impact on cells' capacity to pass through a constriction, increasing or decreasing cell softness, respectively, we aimed at testing whether our device is suitable to highlight the effect of drugs interfering with microtubule organization in cancer cells.

As a microtubule stabilizing agent we used PTX, a member of the taxane family of tubulin-binding drugs, which has anti-motility properties independent of its cytotoxic activity; in fact, at nanomolar concentrations, it reduces cellular motility without threatening cellular viability[31]. To depolymerize microtubules, we used CA-4, an agent that also impairs cellular migration[32,33].

To confirm the biological effects of these drugs in our experimental setting, we exposed MCF7 and MDA-MB231 cells either to 75 nM PTX or to 15 nM CA-4 for 5 hours and we then analysed microtubule organization and cellular migration. By immunofluorescence experiments with an antibody against α-tubulin, we then showed that upon PTX or CA-4 exposure, microtubules lost their radial organization and, after PTX treatment, formed bundles around the nucleus, while following CA-4 treatment, they became short and fuzzy (Fig. 5a). By the wound healing assay, we confirmed the lower migration capacity of MCF7 cells compared to MDA-MB231 cells and we demonstrated that both PTX and CA-4 significantly reduced MDA-MB231 migration (Fig. 5b,c). A reproducible PTX and CA-4 reduction of MCF7 motility was also observed, but it was not significant, probably because of their intrinsic low motility.

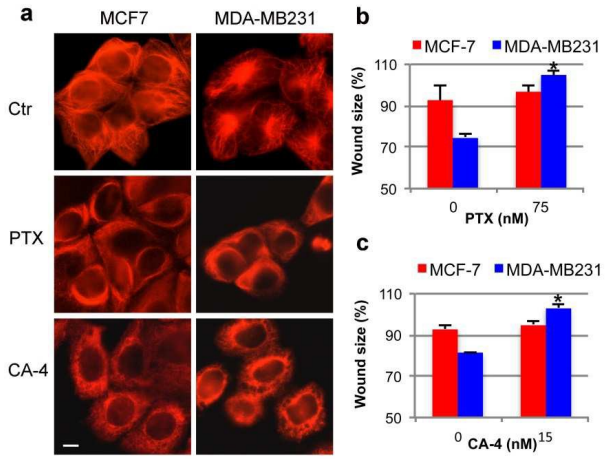

Fig.5 PTX and CA-4 effect on microtubule organization and cell migration in MCF7 and MDA-MB231. Cells were exposed either to 75 nM PTX for 5 hours or to 15 nM CA-4 for 5 hours. (a) Microtubule organization highlighted by indirect immunofluorescence with an anti-α tubulin antibody. Bar: 10 µm. (b) and (c): MCF7 and MDA-MB231 wound sizes after PTX (b) or CA-4 (c) treatment were expressed as percentage of the initial sizes. The results, mean and standard deviation (bars) values, were calculated from three independent experiments (wound size in the treated sample *vs.* its corresponding control sample, *p <0.05).

Before mechanical property analysis, we determined cellular viability of each cell sample using the Trypan blue staining technique and we confirmed that treatments were not cytotoxic, given that less than 1% of the cells appeared blue. Constriction-chip measurements (Fig. 6, detailed results in Table 2) revealed a clear effect of PTX on metastatic MDA-MB231 cells, with passing pressures drastically reduced in treated cells (Fig. 6b). In particular, microtubule stabilization reduced the passing pressure, confirming again that the more rigid a cell is, the more easily it can pass through the constriction, requiring a lower pressure to pass through. In MCF7 cells, we did not observe a significant change in passing pressure values after

PTX treatment (Fig. 6a). This can be explained by two considerations: first the stiffness of MCF7 cells is already quite high, so that probably the impact of PTX is small, and second the passing pressure of untreated cells is already close to the lower boundary of the measurement range, so that further reductions in the passing pressure could be hardly revealed. The analysis of melanoma cells with the constriction chip confirmed that microtubule stabilization has an impact on cells' passage through the constriction. PTX treatment caused a decrease in passing pressures both in A375P and in A375MC2 cells (Fig. 6c, d), although with a greater effectiveness in the most metastatic cells.

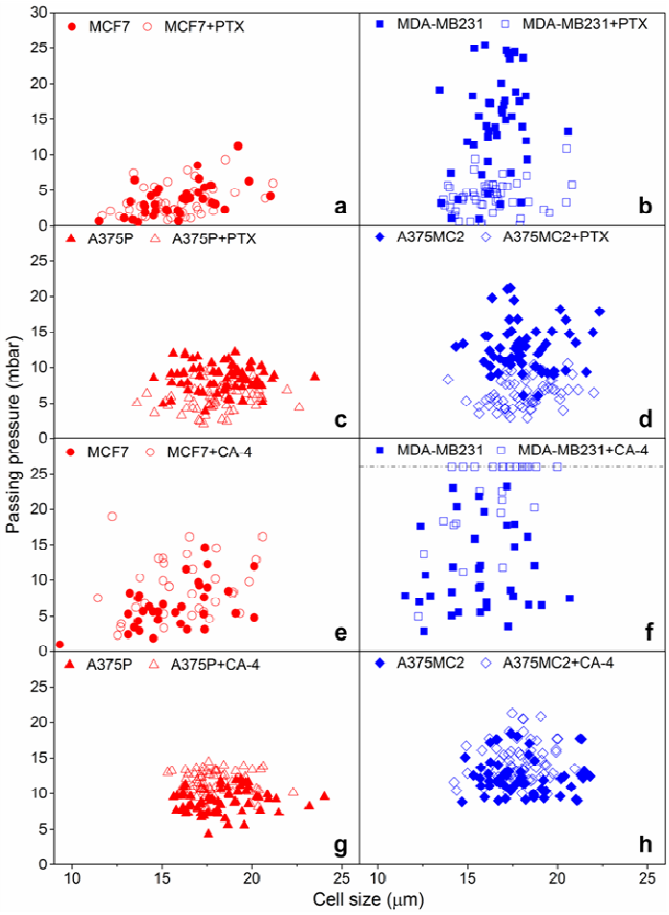

Fig.6 Analysis with the constriction chip of PTX and CA-4 effects on MCF7 (a, e), MDA-MB231 (b, f), A375P (c, g) and A375MC2 (d, h). Cells were exposed to 75 nM PTX (a-d) for 5 hours or to CA-4 (e-h) for 5 hours. The cell size is plotted against pressure values required to push cells through the constriction. The dotted line in panel f represents the maximum measurable pressure.

An opposite result was obtained when breast cancer and melanoma cells were treated with CA-4. In all the four cell lines exposed to the microtubule depolymerizing drug, which is expected to increase cell softness, we indeed found an increase in passing pressures compared to untreated cells (Fig. 6 e-h), indicating that softer cells require higher pressures to pass through the constriction.

It is interesting to highlight that, as can be observed in the scatter diagrams reported in Fig. 3 and 6, within the same cell line, the cell size has almost no impact on passing pressures thus indicating that the measured parameter is mainly related to cell mechanical properties and not to cell size. A different behaviour is exhibited by MCF7 cells (Fig. 3a and Fig. 6a and e): for these cells a positive correlation between the cell size and its passing pressure is observed. This effect, particularly evident for the smallest MCF7 cells, is probably due to the fact that when a cell is small and stiff the role played by its dimensions starts becoming non negligible with respect to that of cell deformation and interaction with the constriction surface.

Table 2. Experimental data for each plot reported in Figure 6. The mean passing pressure with the standard deviation and the median passing pressure are reported for each cell line, together with p values of the statistical analysis (U-test).

Cell line	Passing pressure (mbar)		p value
	Mean ±SD	Median	
MCF7	3.7±2.3	3.4	0.42
MCF7+PTX	3.4±2.1	2.9	
MDA-MB231	14.1±6.9	14.5	<0.001
MDA-MB231+PTX	4.1±2.2	4.1	
A375P	8.6±1.9	8.9	<0.001
A375P+PTX	5.8±1.8	5.8	
A375MC2	12.8±3.3	12.8	<0.001
A375MC2+PTX	6.3±2.0	6.0	
MCF7	4.5±2.1	4.5	<0.001
MCF7+CA-4	8.7±3.8	8.3	
MDA-MB231	11.4±5.9	9.0	<0.001
MDA-MB231+CA-4	21.9±5.8	26	
A375P	9.0±1.7	9.1	<0.001
A375P+CA-4	11.5±1.6	11.4	
A375MC2	12.4±2.6	12.0	<0.001
A375MC2+CA-4	14.3±2.8	13.7	

The results presented so far are summarized in figure 7, where a bar plot of the difference between the passing pressure for each sample with its own control is represented. It is clearly shown that passing pressures depends on cell softness: the softer the cells are, the greater is the resistance to the passage through the constriction and thus also the pressure required to push them through the constriction is higher. Moreover, the results also indicate that the constriction-chip is highly sensitive in highlighting the effect on tumor cells of drugs interfering with microtubule organization. To this regard, it is worth mentioning that we analysed MCF7 and MDA-MB231 cells exposed to PTX with the optical stretcher and we did not find differences in their deformability when compared to their untreated counterparts (see Figure S1 and S2 in supplementary material).

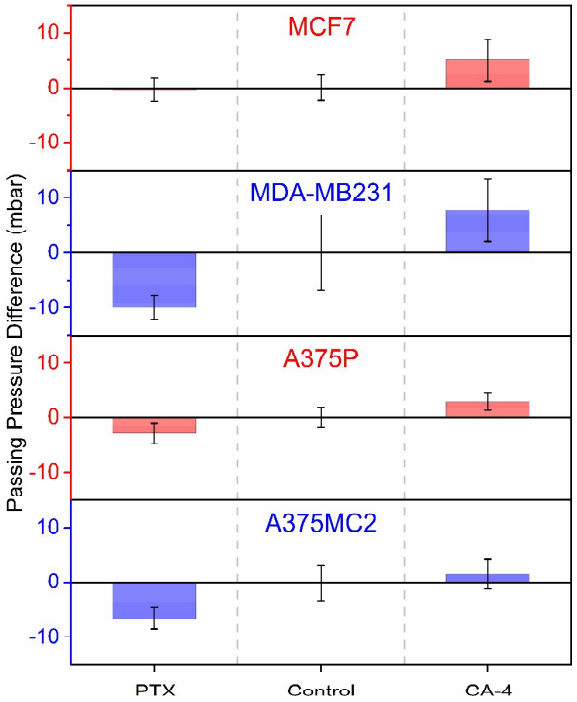

Fig.7 Summary of the obtained results for drug treated cells, passing pressure difference is calculated as the mean value difference between the control sample and the drug-treated one.

A further demonstration of the suitability of the constriction chip to study changes in cellular deformability was obtained by analysing cells' response to nocodazole. This drug is known to interfere with microtubule organization in a concentration dependent manner: at low nanomolar concentrations it stabilizes microtubules by interfering with their dynamics, while at high micromolar concentrations it induces microtubules depolymerisation[34-37]. Thus, we tested the impact on breast cancer and melanoma cells' passage through the constriction of treatments with either a low (200 nM for 4 hours) or a high nocodazole concentration (33 μM for 1 hour). By Trypan blue staining, we found that after treatment with either one or the other drug concentration cellular viability was not impaired. As shown in Fig. 8, the pressure values decreased for MDA-MB231 and A375MC2 high metastatic cells treated with a low nocodazole concentration, while they increased in all the cell lines exposed to a high concentration of nocodazole. Thus, these results indicate that the different nocodazole concentrations, causing opposite effects on microtubule organization, determine an opposite cell mechanical behaviour, which is easily detectable by the constriction chip.

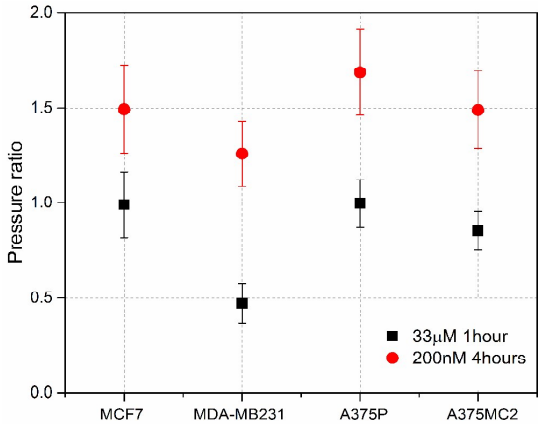

Fig.8 Nocodazole effect on cancer cell passage through a constriction. The ratio between the average passing-pressure of treated and untreated cells is reported for both the low-concentration and high-concentration treatment, for all the considered cell lines.

Conclusions

In this work, we have reported the fabrication and validation of a new integrated microfluidic device that allows evaluating cellular deformability on the basis of the pressure required to make cells pass through a constriction.

Using cancer cell lines endowed with different metastatic potential, we have shown that the device can easily distinguish cells at different stages of cancer progression. In fact, within each pair of cell lines, cells with the higher metastatic potential required higher pressures to pass through the constriction than the less metastatic or non-metastatic ones. The higher pressure required by MDA-MB231 cells to pass through the constriction compared to MCF7 cells was paralleled by a greater deformability, as measured by an optical stretcher, indicating that passing pressures increase with an increase in cell softness. The results obtained by exposing cells to PTX, CA-4 or nocodazole indicate that microtubules play an important role in determining the ability of a cell to pass through a constriction; moreover, they confirm the inverse relationship between cell softness and passing pressures in our device. In fact, PTX and low nocodazole concentrations, which stabilize microtubules and make cell stiffer, leading to a clear decrease in passing pressures. On the contrary, CA-4 and high nocodazole concentrations, depolymerizing microtubules, cause an increase in cell softness and an increase in passing pressures.

Taken together, the results presented here indicate that the constriction-chip is a valid tool to study cellular mechanical properties in relationship to metastatic potential, as well as in response to drug treatment. It can give reliable results analysing a very small number of cells, less than 100, and could therefore be particularly useful when the number of cells available is limited. Moreover, the analysis can be fast, since measurements of about 100 cells require a few hours, as well as results elaboration. In addition, the constriction-chip, analysing deformability at the single cell level, can give information on

the possible heterogeneity of a cell population, as detected in MDA-MB231 and A375MC2 cells. Given the low number of cells required for the analysis, a further development of this device could lead to its possible use to study cancer progression and the response to therapies of cancer cells obtained by tumour biopsies. A limitation of this device is that the constriction size must be smaller than the dimensions of the cells under examination, thus a panel of devices with different constriction sizes should be available for the analysis of cells characterized by different dimensions. It is worth noticing that this device does not aim to simulate *in vivo* cancer cell migration behaviour, it is designed to be an analysis device to distinguish between cancer cells with different metastatic potential and to evidence the effect of drugs possibly interfering with cellular deformability.

In conclusion, the constriction-chip that we developed represents a new device for the study of cellular mechanical characteristics, which could be exploited to investigate cellular properties in relationship to different biological processes.

Acknowledgements

We acknowledge Fondazione Cariplo for the financial support through the grant ‘‘Optofluidic chips for the study of cancer cell mechanical properties and invasive capacities’’ (Ref. # 2011-0370). The authors thank Dr. Richard Hynes (Howard Hughes Medical Institute, Center for Cancer Research, MIT) for the generous gift of A375 and A375MC2 cells and Prof. G. Dubini for interesting discussions. The authors from University of Pavia would like to thank Alice Pietra for her precious help in the cell measurements and in the identification of a proper statistical analysis method.

Notes and references

[a] Istituto di Fotonica e Nanotecnologie (IFN)-CNR,Piazza Leonardo da Vinci 32, 20133 Milano, Italy

[b] Dipartimento di Ingegneria Industriale e dell’Informazione, Università di Pavia, Via Ferrata 5A, 27100 Pavia, Italy.

[c] Istituto di Genetica Molecolare (IGM)-CNR, Via Abbiategrasso 207, 27100 Pavia, Italy.

[d] Laboratory of Biological Structure Mechanics - LaBS Department of Chemistry, Materials and Chemical Engineering ‘Giulio Natta’, Politecnico di Milano, Piazza Leonardo da Vinci 32, 20133 Milano, Italy

† These authors contributed equally to the work.

* Corresponding author. Email: mondello@igm.cnr.it, Tel: +39-0382985207.

Electronic Supplementary Information (ESI) available: See DOI: 10.1039/b000000x/

1 S. Suresh, *Acta Biomater.,* 2007, **3**, 413-438.

2 S. Kumar, V.M. Weaver, *Cancer Metastasis Rev.*, 2009, **28**, 113-127.

3 J. Guck, F. Lautenschläger, S. Paschke, M. Beil*, Integr Biol*., 2010, **2**, 575-583.

4 V. Swaminathan, K. Mythreye, E.T. O'Brien, A. Berchuck, G.C. Blobe , R. Superfine, *Cancer Res*., 2011, **71**, 5075-5080.

5 Alberts B, Johnson A, Lewis J, Raff M, Roberts K, Walter P, Molecular Biology of the Cell. Garland Science, New York, 2007.

6 C. Rotsch, M. Radmacher, *Biophys J.*, 2000, **78**, 520-535.

7 J. Guck, S. Schinkinger, B. Lincoln, F. Wottawah, S. Ebert, M. Romeyke, D. Lenz, H. M. Erickson, R. Ananthakrishnan, D. Mitchell, J. Käs, S. Ulvick and C. Bilby, *Biophys J.*, 2005, **88**, 3689-3698.

8 B. Lincoln, F. Wottawah, S. Schinkinger, S. Ebert and J. Guck, *Methods Cell Biol.*, 2007, **83**, 397-423.

9 C.G. Rolli, T.Seufferlein, R. Kemkemer and J.P. Spatz, *PLoS One*, 2010, **5**, e8726.

10 H. Yun, K. Kim and W.G. Lee, *Biofabrication*, 2013, **5**, 022001.

11 V. Lecault, A. K. White, A. Singhal and C.L. Hansen, *Curr Opin in Chem Biol.*, 2012, **16**, 381-390.

12 B. Lincoln, S. Schinkinger, K. Travis, F. Wottawah, S. Ebert, F. Sauer and J. Guck, *Biomed Microdevices*, 2007, **9**, 703-710.

13 M. Mak, C. A. Reinhart-King and D. Erickson, *Lab Chip*, 2013, **13**, 340-348.

14 A.E. Ekpenyong , G. Whyte, K. Chalut, S. Pagliara, F. Lautenschläger , C. Fiddler, S. Paschke, U. F. Keyser, E. R. Chilvers and J. Guck, *PLoS ONE*, 2012, **7**, e45237.

15 J. Guck, R. Ananthakrishnan, H. Mahmood, T.J. Moon, C.C. Cunningham and J. Käs, *Biophysical J.*, 2001, **81**, 767-784.

16 J. Männik, R. Driessen, P. Galajda, J. E. Keymer, C. Dekker, *Proc Natl Aca. Sci USA*, 2009, **106**, 14861-14866.

17 Q. Guo, S. Park and H. Ma, *Lab Chip*, 2012, **12**, 2687-2695.

18 S. Gabriele, M. Versaeel, P. Pereira and O. Théodoly, *Lab Chip*, 2010, **10**, 1459-1467.

19 F. Lautenschläger, S. Paschke, S. Schinkinger, A. Bruel, M. Beil, and J. Guck, *Proc Natl Aca. Sci USA,* 2009, **106**, 15696-15701.s

20 P. Preira, M-P Valignat, J. Bico and O. Théodoly, *Biomicrofluidics*, 2013, **7**, 024111.

21 H.W. Hou, Q.S. Li, G.Y.Lee, A.P. Kumar, C.N. Ong and C.T. Lim, *Biomed Microdevices*. 2009, **11**, 557-564.

22 N. Bellini, F. Bragheri, I. Cristiani, J. Guck, R. Osellame, and G. Whyte, *Biomed Opt Express*, 2012, **3**, 2658-2668.

23 F. Bragheri, P. Minzioni, R. Martinez Vazquez, N. Bellini, P. Paie, C. Mondello, R. Ramponi, I. Cristiani and R. Osellame, *Lab Chip*, 2012, **12**, 3779–3784.

24 T. Yang, P. Paiè, G. Nava, F. Bragheri, R. Martinez Vazquez, P. Minzioni, M. Veglione, M. Di Tano, C. Mondello, R. Osellame and I. Cristiani, Lab Chip, 2015, DOI: 10.1039/c4lc01496k.

25 N. Bellini, K. C. Vishnubhatla, F. Bragheri, L. Ferrara, P. Minzioni, R. Ramponi, I. Cristiani, and R. Osellame, *Opti Express*, 2010, **18**, 4679-4688.

26 B.E. Bachmeier, A.G. Nerlich, R. Lichtinghagen, C.P. Sommerhoff, *Anticancer Res.*, 2001, **21**, 3821-3828.

27 H.D. Soule, J. Vazguez, A. Long, S. Albert and M.A. Brennan, *J Natl Cancer Inst.*, 1973, **51**, 1409-1416.

28 L. Xu, S. Begum, J.D. Hearn, R.O. Hynes, *Proc Natl Acad Sci USA.*, 2006, **103**, 9023-9028.

29 F. Gittes, B. Mickey, J. Nettleton and J. Howard, *J Cell Biol.*, 1993, **120**, 923–934.

30 R. Giavazzi, K. Bonezzi and G. Taraboletti, *Microtubules as targets for Cancer Therapies*, T Fojo (Ed), Humana Press, Totowa, NJ., 2008, pp. 519-530.

31 K. Bonezzi, D Belotti, B.J. North, C. Ghilardi, P. Borsotti, A. Resovi, P. Ubezio, A. Riva, R. Giavazzi, E. Verdin and G. Taraboletti, *Neoplasia*, 2012, **14**, 846-854.

32 C.H. Shen, J.J. Shee, J.Y. Wu, Y.W. Lin, J.D. Wu and Y.W. Liu, *Br J Pharmacol.*, 2010, **160**, 2008-2027.

33 Y. Lu, J. Chen, M. Xiao, W. Li and D.D. Miller, *Pharm Res.*, 2012, **29**, 2943-2971.

34 M.A. Jordan, D. Thrower and L Wilson, *J Cell Sci.*, 1992, **102**, 401-416.

35 R.J. Vasquez, B. Howell, A.M. Yvon, P. Wadsworth and L. Cassimeris, *Mol Biol Cell*., 1997, **8**, 973-985.

36 P.A. Friedman and E.G. Platzer, *Biochim Biophys Acta*, 1978, **544**, 605-614.

37 F. Frezzato, V. Trimarco, V. Martini, C. Gattazzo, E. Ave, A. Visentin, A. Cabrelle, V. Olivieri, R. Zambello, M. Facco, F. Zonta, A. Cristiani, A.M. Brunati, S. Moro, G. Semenzato and L. Trentin, *Br J Haematol*., 2014, **165**, 659-672.